Do System Impedances Really Affect Power Swings – Applying Power Swing Protection Elements Without Complex System Studies

Normann Fischer, Gabriel Benmouyal, Daqing Hou,
Demetrios Tziouvaras, John Byrne-Finley, and Brian Smyth
Schweitzer Engineering Laboratories, Inc.

This paper was presented at the 65th Annual Conference for Protective Relay Engineers and can be accessed at: http://dx.doi.org/10.1109/CPRE.2012.6201225.

For the complete history of this paper, refer to the next page.

Presented at the
12th Annual Clemson University Power Systems Conference
Clemson, South Carolina
March 12–15, 2013

Previously presented at the
66th Annual Georgia Tech Protective Relaying Conference, April 2012

Previous revised edition released April 2012

Originally presented at the
65th Annual Conference for Protective Relay Engineers, April 2012

Do System Impedances Really Affect Power Swings – Applying Power Swing Protection Elements Without Complex System Studies

Normann Fischer, Gabriel Benmouyal, Daqing Hou, Demetrios Tziouvaras, John Byrne-Finley, and Brian Smyth,
Schweitzer Engineering Laboratories, Inc.

***Abstract*—One of the traditional techniques for detecting power swings uses a dual-quadrilateral characteristic. It is based on the measurement of the time interval it takes the positive-sequence impedance to cross two blinders. Another technique monitors the variation of the swing center voltage approximation. This paper presents a performance comparison between applications of these two techniques in cases derived from a sample network transient simulation and in cases recorded during real operations in the field.**

I. Introduction

A balance between generated and consumed active power exists during steady-state operating conditions and is necessary for the stability of the power system. Power system disturbances cause oscillations in machine rotor angles that can result in severe power flow swings. Depending on the severity of the disturbance and the actions of power system controls, the system may remain stable or experience a large separation of generator rotor angles and eventually lose synchronism. Large power swings can cause unwanted relay operations that can further aggravate the power system disturbance and cause major power outages or blackouts.

A power swing blocking (PSB) function is available in modern distance relays to prevent unwanted distance relay element operation during power swings.

Traditional PSB and out-of-step tripping (OST) functions may use dual-quadrilateral characteristics that are based on the measurement of the time interval it takes the positive-sequence impedance to cross the two blinders. An extensive number of power system stability studies may be required, taking into consideration different operating conditions, in order to determine the settings for the dual-quadrilateral PSB and OST functions. This is a costly exercise, and we can never be certain that all possible scenarios and operating conditions were considered.

The swing center voltage (SCV) method calculates the positive-sequence SCV rate of change and does not require any stability studies or user settings for the proper blocking of relay elements. This method is well suited for long, heavily loaded transmission lines that pose significant problems for traditional power swing detection methods.

This paper presents a performance comparison between the traditional dual-quadrilateral method and the SCV variation method. The performances of both methods are analyzed using field data obtained from a system disturbance and transient simulation data obtained from a Real Time Digital Simulator (RTDS®).

II. Power Swings and Out-of-Step Phenomenon

A power swing is a system phenomenon that is observed when the phase angle of one power source starts to vary in time with respect to another source on the same network. The phenomenon generally occurs following a major disturbance, like a fault, that alters the mechanical equilibrium of one or more machines. A power swing is stable when, following a disturbance, the rotation speed of all machines returns to synchronous speed. A power swing is unstable when, following a disturbance, one or more machines do not return to synchronous speed, thereby losing synchronism with the rest of the system.

A. Basic Phenomenon Using the Two-Source Model

The simplest network for studying the power swing phenomenon is the two-source model, as shown in Fig. 1. The left source has a phase angle advance equal to θ, and this angle will vary during a power swing. The right source represents an infinite bus, and its angle will not vary with time. As simple as it is, this elementary network can be used to model the phenomena taking place in more complex networks.

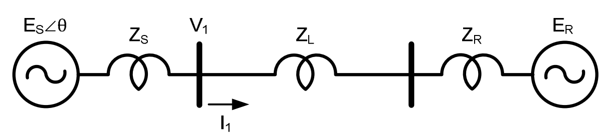

Fig. 1. Two-source equivalent elementary network

B. Representation of Power Swings in the Impedance Plane

Assuming the sources have equal amplitude, for a particular phase angle θ, the location of the positive-sequence impedance (Z_1) calculated at the left bus is provided by the following equation [1].

$$Z_1 = \frac{V_1}{I_1} = Z_T \bullet \frac{E_S\angle\theta}{E_S\angle\theta - E_R} - Z_S \tag{1}$$

In (1), Z_T is the total impedance, as in:

$$Z_T = Z_S + Z_L + Z_R \tag{2}$$

Assuming the two sources are of equal magnitude, the Z_1 impedance locus in the complex plane is given by (3).

$$Z_1 = \frac{Z_T}{2} \bullet \left(1 - j\cot\frac{\theta}{2}\right) - Z_S \tag{3}$$

When the angle θ varies, the locus of the Z_1 impedance is a straight line that intersects the segment Z_T orthogonally at its middle point, as shown in Fig. 2. The intersection occurs when the angular difference between the two sources is 180 degrees.

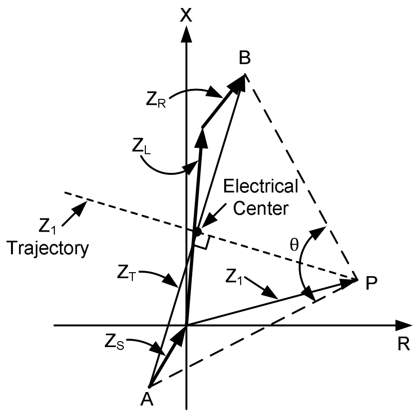

Fig. 2. Locus of the Z_1 impedance during a power swing with sources of equal magnitude

When the two sources have unequal magnitudes such that *n* is the ratio of E_S over E_R, the locus of the Z_1 impedance trajectory will correspond to the circles shown in Fig. 3. For any angle θ, the ratio of the two segments joining the location of the extremity of Z_1 (point P) to the total impedance extremities A and B is equal to the ratio of the source magnitudes:

$$n = \frac{E_S}{E_R} = \frac{PA}{PB} \tag{4}$$

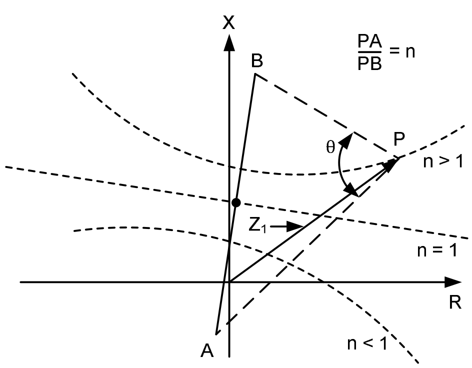

Fig. 3. Locus of the Z_1 impedance during a power swing with sources of unequal magnitudes

The precise equation for the center and radius of the circles as a function of the ratio *n* can be found in [1].

It should be noted that, in reality, a power source is a synchronous generator and is therefore not an ideal voltage source as represented in the two-source model. Furthermore, the impact of any existing automatic voltage regulator must be considered. During a power swing, the ratio of two power source magnitudes is not going to remain constant. Therefore, the resulting locus of the Z_1 impedance will switch from one circle to another depending upon the instantaneous magnitude ratio [2].

C. Rate of Change of the Positive-Sequence Impedance

Starting with (1) and assuming the two sources are of equal magnitude, the time derivative of the Z_1 impedance is provided by (5).

$$\frac{dZ_1}{dt} = -jZ_T \bullet \frac{e^{-j\theta}}{\left(1 - e^{-j\theta}\right)^2} \bullet \frac{d\theta}{dt} \tag{5}$$

Assuming the phase angle has a linear variation with a slip frequency in radians per second given as:

$$\frac{d\theta}{dt} = \omega \tag{6}$$

and using the identity:

$$\left|1 - e^{-j\theta}\right| = 2 \bullet \sin\frac{\theta}{2} \tag{7}$$

the rate of change of the Z_1 impedance is finally expressed as:

$$\left|\frac{dZ_1}{dt}\right| = \frac{|Z_T|}{4 \bullet \sin^2\frac{\theta}{2}} \bullet |\omega| \tag{8}$$

Equation (8) expresses the principle that the rate of change of the Z_1 impedance depends upon the sources, transmission line impedances, and the slip frequency, which, in turn, depends upon the severity of the perturbation.

As a consequence, any algorithm that uses the Z_1 impedance displacement speed in the complex plane to detect a power swing will depend upon the network impedances and the nature of the perturbation. Furthermore, contrary to the positive-sequence line impedance, the source impedances are not introduced into the relay so the relay cannot usually predict the displacement speed.

Fig. 4 shows the normalized plot of the rate of change of the Z_1 impedance as a function of the phase angle θ. The minimum value is 1, corresponding to θ equals 180 degrees. In order to get the real value of the rate of change, the vertical axis has to be multiplied by:

$$\frac{|Z_T|}{4} \bullet |\omega| \tag{9}$$

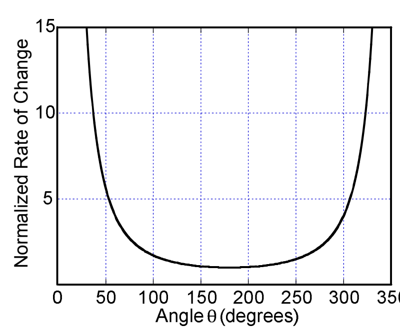

Fig. 4. Normalized rate of change of the Z_1 impedance

Fig. 4 also shows that the higher the total impedance (Z_T) and slip frequency, the higher the minimum value of the Z_1 impedance rate of change. Note that the region of importance for PSB and OST is the flat segment of the curve in Fig. 4.

D. The Justification for Detecting Power Swings

There are two reasons why power swings should be detected. First, they can lead to the misoperation of some protection elements, such as Zone 1 distance, phase overcurrent, or phase undervoltage. For these instances, a PSB signal is needed to ensure the security of these elements. Second, in the case of an unstable swing, a network separation is needed in order to avoid a network collapse. In this instance, the out-of-step (OOS) condition must be detected in order to generate an OST signal.

III. The Dual-Quadrilateral Technique (Method A)

A. Basic Principle

The dual-quadrilateral technique for detecting power swings uses the rate of change of the Z_1 impedance. It is based on the principle that the Z_1 impedance variation is gradual during a power swing, because of the system generator inertias, while it is virtually a step change with a short time constant during a fault.

Both faults and power swings may cause the Z_1 impedance to enter into the operating characteristic of a distance element. The impedance measurement by the distance element alone cannot be used to distinguish a power swing from a fault. The dual-quadrilateral method discriminates between faults and power swings by calculating the rate of change of the Z_1 impedance. Fig. 5 shows the dual-quadrilateral impedance-based characteristic used for detecting power swings on a power system.

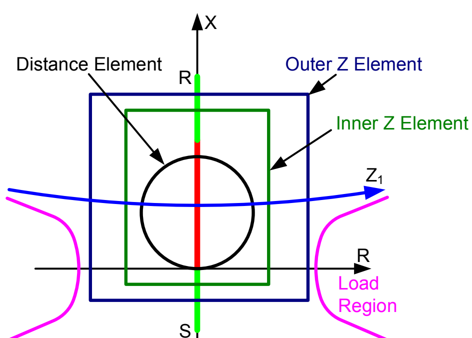

Fig. 5. Quadrilateral impedance-based power swing detection characteristic

The actual implementation of measuring the Z_1 impedance rate of change is typically performed by measuring the time it takes the Z_1 impedance to traverse through the dual-quadrilateral elements. A timer is started when the Z_1 impedance enters the outer characteristic (see Fig. 5). If the Z_1 impedance remains between the inner and outer characteristics for the set time delay, the PSB element operates and selected distance element zones are blocked from operation for a period of time.

B. Issues Associated With the Dual-Quadrilateral Method

1) Impact of the System Impedances on the PSB Function

To guarantee enough time to carry out blocking of the distance elements after a power swing is detected, the inner impedance of the dual-quadrilateral element must be placed outside the largest distance element for which blocking is required. In addition, the outer dual-quadrilateral impedance element must be placed away from the load region to prevent PSB logic operation caused by heavy loads, thus establishing an incorrect blocking of the line mho tripping elements. This is illustrated in Fig. 5.

The previous requirements are difficult to achieve in some applications, depending on the relative line impedance and source impedance magnitudes [3]. Fig. 6 shows a simplified representation of one line interconnecting two generating sources in the complex plane with a swing locus bisecting the total impedance. Fig. 6a depicts a system in which the line impedance is large compared with system impedances (strong source), and Fig. 6b depicts a system in which the line impedance is much smaller than the system impedances (weak source).

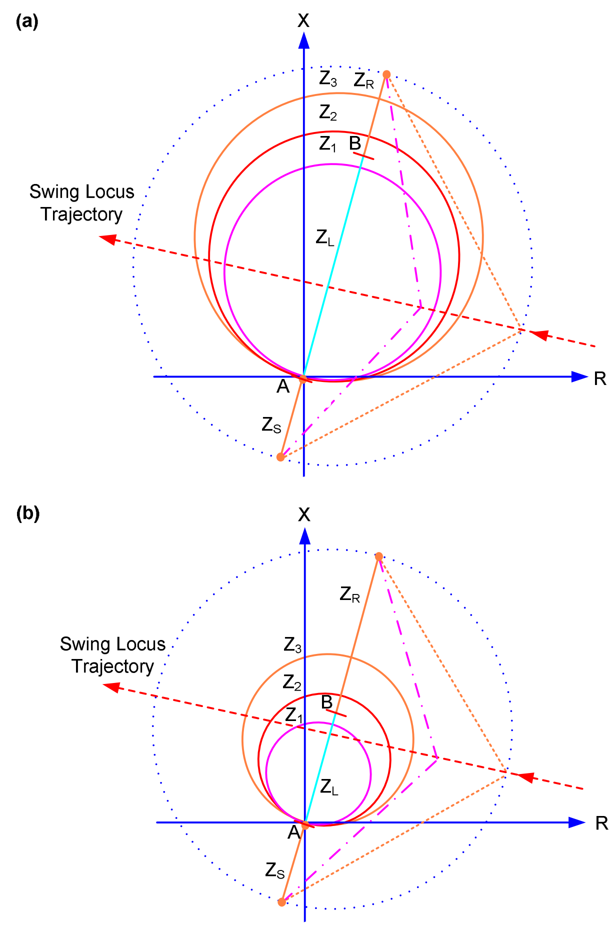

Fig. 6. Effects of source and line impedances on the PSB function

We can observe from Fig. 6a that the swing locus could enter the Zone 2 and Zone 1 relay characteristics during a stable power swing from which the system could recover. For this particular system, it may be difficult to set the inner and outer PSB quadrilateral elements, especially if the line is heavily loaded, because the necessary PSB settings are so large that the load impedance could establish incorrect blocking. To avoid incorrect blocking resulting from load, lenticular distance relay characteristics, or blinders that restrict the tripping area of the mho elements, were applied in the past. On the other hand, the system shown in Fig. 6b becomes unstable before the swing locus enters the Zone 2 and Zone 1 mho elements, and it is relatively easy to set the inner and outer PSB quadrilateral elements.

Another difficulty with the dual-quadrilateral method is the separation between the inner and outer PSB quadrilateral elements and the timer setting that is used to differentiate a fault from a power swing. The above settings are not difficult to calculate, but depending on the system under consideration, it may be necessary to run extensive stability studies to determine the fastest power swing and the proper PSB quadrilateral element settings. The rate of slip between two systems is a function of the accelerating torque and system inertias. In general, a relay cannot determine the slip analytically because of the complexity of the power system. However, by performing system stability studies and analyzing the angular excursions of systems as a function of time, we can estimate an average slip in degrees per second or cycles per second. This approach may be appropriate for systems where slip frequency does not change considerably as the systems go out of step. However, in many systems where the slip frequency increases considerably after the first slip cycle and on subsequent slip cycles, a fixed impedance separation between the dual-quadrilateral elements and a fixed time delay may not be suitable to provide a continuous blocking signal to the mho distance elements.

In a complex power system, it is very difficult to obtain the proper source impedances that are necessary to establish the blinder and PSB delay timer settings [4]. The source impedances vary continuously according to network changes, such as additions of new generation and other system elements. The source impedances could also change drastically during a major disturbance and at a time when the PSB and OST functions are called upon to take the proper actions. Note that the design of the PSB and OST functions would have been trivial if the source impedances remained constant and if it were easy to obtain them. Normally, very detailed system stability studies are necessary to consider all contingency conditions in determining the most suitable equivalent source impedance to set the dual-quadrilateral PSB or OST functions.

2) *Impact of Heavy Load on the Resistive Settings of the Quadrilateral Element*

References [4] and [5] recommend setting the concentric dual-quadrilateral power swing characteristics inside the maximum load condition but outside the maximum distance element reach desired to be blocked. In long line applications with a heavy load flow, following these settings guidelines may be difficult, if not impossible. Fortunately, most numerical distance relays allow some form of programming capability to address these special cases. However, in order to set the relay correctly, stability studies are required; a simple impedance-based solution is not possible.

The approach for this application is to set the power swing blinder such that it is inside the maximum load flow impedance and the worst-case power swing impedance, as shown in Fig. 7. Using this approach may result in cutting off part of the distance element characteristic. Reference [6] provides additional information and logic to address the issues of PSB settings in heavily loaded transmission lines.

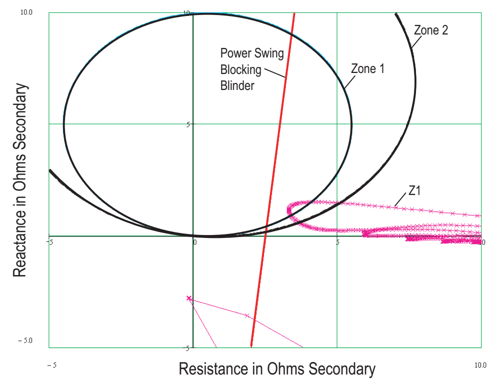

Fig. 7. Impedance plane plot of a high-load PSB scheme

IV. The Swing Center Voltage Variation Method (Method B)

A. *Swing Center Voltage*

Swing center voltage is defined as the voltage at the location of a two-source equivalent system where the voltage value is zero when the angles between the two sources are 180 degrees apart. Fig. 8 illustrates the voltage phasor diagram of a general two-source system, with the SCV shown as the phasor from origin *o* to the point *o′*.

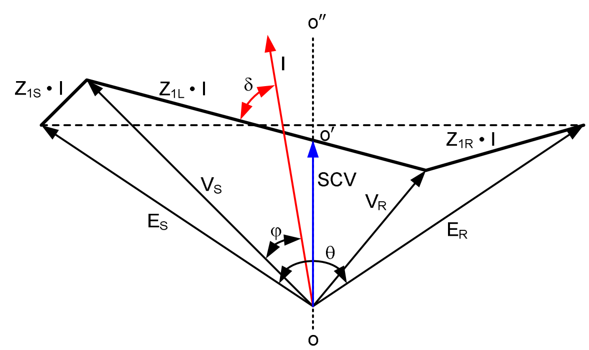

Fig. 8. Voltage phasor diagram of a two-source system

When a two-source system loses stability and enters an OOS condition, the angle difference of the two sources, θ(t), will increase as a function of time. As derived in detail in [3], we can represent the SCV by (10), assuming an equal source magnitude, E.

$$\mathrm{SCV}(t) = \sqrt{2}E\sin\left(\omega t + \frac{\theta(t)}{2}\right)\bullet\cos\left(\frac{\theta(t)}{2}\right) \qquad (10)$$

SCV(t) is the instantaneous SCV that is to be differentiated from the SCV that the relay estimates. Equation (10) is a typical amplitude-modulated sinusoidal waveform. The first sine term is the base sinusoidal wave, or the carrier, with an average frequency of ω + (1/2)(dθ/dt). The second term is the cosine amplitude modulation.

Fig. 9 shows a positive-sequence SCV (SCV1) for a power system with a nominal frequency of 50 Hz and a constant slip frequency of 5 Hz. When the frequency of a sinusoidal input is different from that assumed in its phasor calculation, as is in the case of an OOS situation, oscillations in the phasor magnitude result. However, the amplitude calculation in Fig. 9 is smooth because the positive-sequence quantity effectively averages out the amplitude oscillations of individual phases.

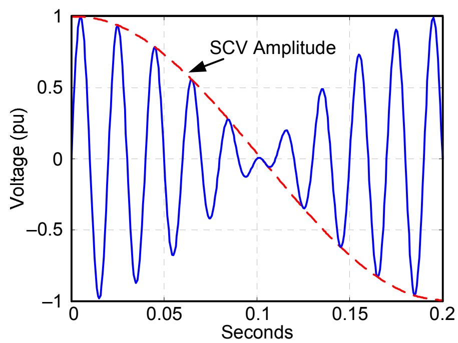

Fig. 9. SCV during an OOS condition

The magnitude of the SCV changes between 0 and 1 per unit of system nominal voltage. With a slip frequency of 5 Hz, the voltage magnitude is forced to 0 every 0.2 second. Fig. 9 shows the SCV during a system OOS condition. Under normal load conditions, the magnitude of the SCV stays constant.

B. Swing Center Voltage Approximation in the Form of the Ilar Voltage

One popular approximation of the SCV obtained through the use of locally available quantities is as follows:

$$\mathrm{SCV} \approx |V_S| \bullet \cos\varphi \tag{11}$$

where:

$|V_S|$ is the magnitude of locally measured voltage.

φ is the angle difference between V_S and the local current, as shown in Fig. 10.

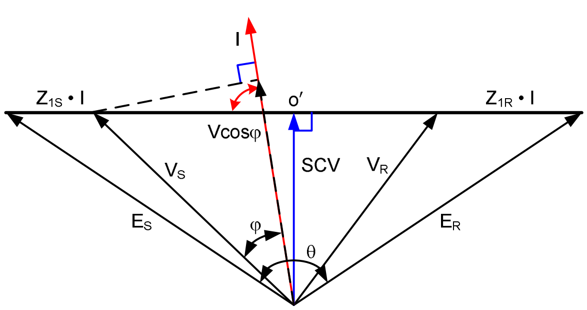

Fig. 10. Vcosφ is a projection of local voltage, V_S, onto local current, I

In Fig. 10, we can see that Vcosφ is a projection of V_S onto the axis of the current, I. For a homogeneous system with the system impedance angles close to 90 degrees, Vcosφ approximates well the magnitude of the SCV. For the purpose of power swing detection, it is the rate of change of the SCV that provides the main information of system swings. Therefore, some difference in magnitude between the system SCV and its local estimate has little impact in detecting power swings. We will, therefore, refer to Vcosφ as the SCV in the following discussion. The quantity of Vcosφ was first introduced by Ilar for the detection of power swings [7].

Using (10) and keeping in mind that the local SCV is estimated using the magnitude of the local voltage, V_S, the relation between the SCV and the phase angle difference, θ, of two source voltage phasors can be simplified to the following:

$$\mathrm{SCV1} = \mathrm{E1} \bullet \cos\left(\frac{\theta}{2}\right) \tag{12}$$

In (12), E1 is the positive-sequence magnitude of the source voltage, E_S, shown in Fig. 10 and is assumed to be also equal to E_R. We use SCV1 in power swing detection for the benefit of its smooth amplitude during a power swing on the system. The magnitude of the SCV is at its maximum when the angular difference between the two sources is zero. Conversely, it is at its minimum (or zero) when the angular difference between the two sources is 180 degrees. This property has been exploited so that a power swing can be detected by calculating the rate of change of the SCV. The time derivative of SCV1 is given by (13).

$$\frac{d(\mathrm{SCV1})}{dt} = -\frac{\mathrm{E1}}{2}\sin\left(\frac{\theta}{2}\right)\frac{d\theta}{dt} \tag{13}$$

Equation (13) provides the relationship between the rate of change of the SCV and the two-machine system slip frequency, dθ/dt. Equation (13) shows that the derivative of SCV1 is independent of power system impedances. Fig. 11 is a plot of SCV1 and the rate of change of SCV1 for a system with a constant slip frequency of 1 radian per second.

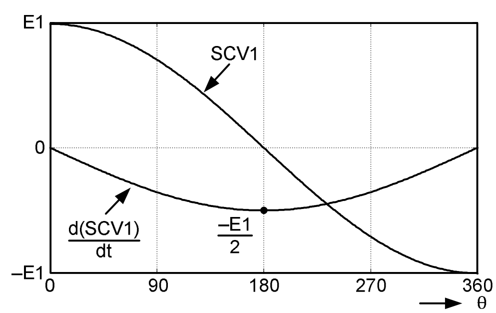

Fig. 11. SCV1 and its rate of change with unity source voltage magnitudes

Before ending this section, we want to point out the following two differences between the system SCV and its local estimate (these magnitude differences do not impact the power swing detection, which is based primarily on the rate of change of the SCV):

1. When there is no load flowing on a transmission line, the current from a line terminal is basically the line charging current that leads the local terminal voltage by approximately 90 degrees. In this case, the local estimate of the SCV is close to zero and does not represent the true system SCV.

2. The local estimate of the SCV has a sign change in its value when the difference angle, θ, of two equivalent sources goes through 0 degrees. This sign change results from the reversal of the line current (i.e., φ changes 180 degrees when θ goes through the 0-degree point). The system SCV does not have this discontinuity.

C. Independence of the Swing Center Voltage Variation From the System Impedances

As shown in (12), the SCV is independent of the system source and line impedances and is, therefore, particularly attractive for use in a no-setting power swing detection function. Other quantities, such as the resistance and its rate of change and the real power and its rate of change, depend on the line and system source impedances and other system parameters that make them less suitable for use in a no-setting power swing function.

V. Comparison Between Method A and Method B

A. Simulation Examples of Power Swing Detection Using Methods A and B

The two methods, dual-quadrilateral and SCV, operate on different principles but ultimately arrive at the same result. This section presents a comparison of the two methods as they apply to a two-source power system. The power system used for the comparison consists of two strong sources connected through a parallel transmission line (see Fig. 12). The power system is built in an RTDS environment. The simulated data are played back to a relay having either the dual-quadrilateral or the SCV PSB method enabled.

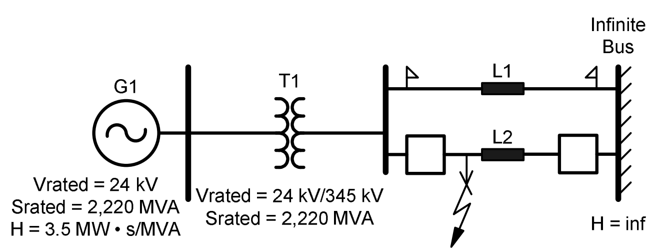

Fig. 12. Power system simulation model

To create the power swing, a three-phase fault is placed on Line L2 close into the bus but cleared after a set delay. The fault and the delay of the fault clearing cause the power swing and also determine if the swing will be stable or unstable. The power swing is monitored on Line L1 while the breakers are open on Line L2. Reclosing is also implemented to close L2 back into service 1 second after the breakers are tripped. Reclosing does not impact the operation of the PSB detection. When the previously faulted line is switched back into service, the line immediately picks up load, thereby reducing load current in the unfaulted line. This appears as an increase in impedance when viewed from the unfaulted line. However, from the power system point of view, the overall impedance is decreased (the two lines are now once again in parallel) and the power transfer capability of the system is increased, therefore increasing the generator stability.

To test the operation of both PSB detection methods, stable and unstable swings are produced from the simulation. The generator in the simulation model is equipped with both an automatic voltage regulator and a power system stabilizer, but for the cases presented here, both are turned off.

For a stable swing, the swing rate is approximately 1.2 Hz (see Fig. 13). The positive-sequence impedance for the stable swing is shown in Fig. 14. At 100 cycles, L2 is reclosed. When L2 is closed back in, the L1 current decreases because L2 carries half of the load. This appears as an increase of impedance on the relay that monitors L1 voltages and currents.

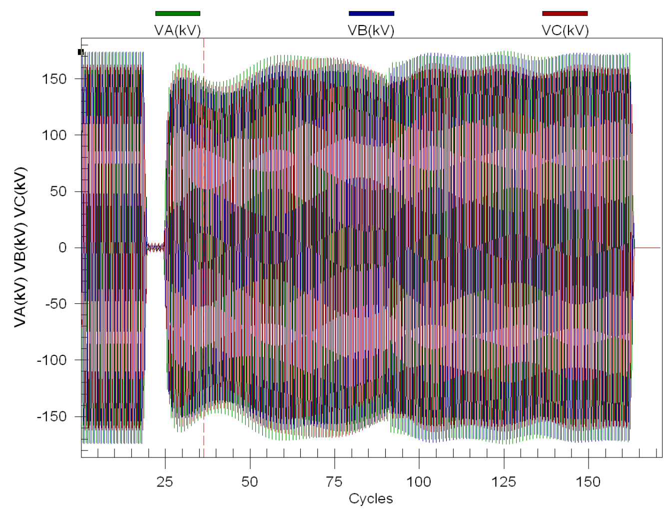

Fig. 13. Stable power swing

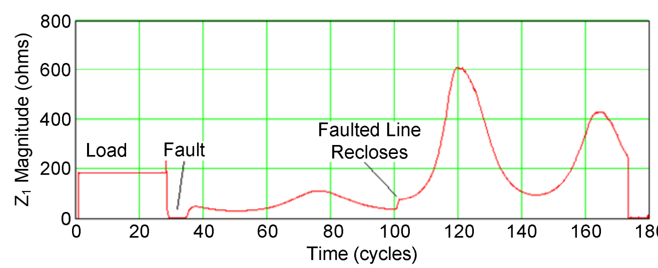

Fig. 14. Impedance plot for the stable power swing

The unstable swing is about 4.5 Hz with an increasing swing rate up to 8.5 Hz (see Fig. 15). The positive-sequence impedance for the unstable swing is plotted in Fig. 16. Similar to the stable swing, the reclosing occurs at 100 cycles, decreasing the system impedance and increasing power transfer capability. Both of these simulation cases are saved as Common Format for Transient Data Exchange (COMTRADE) files and played back to the relay through a test set to see how the PSB logic will behave.

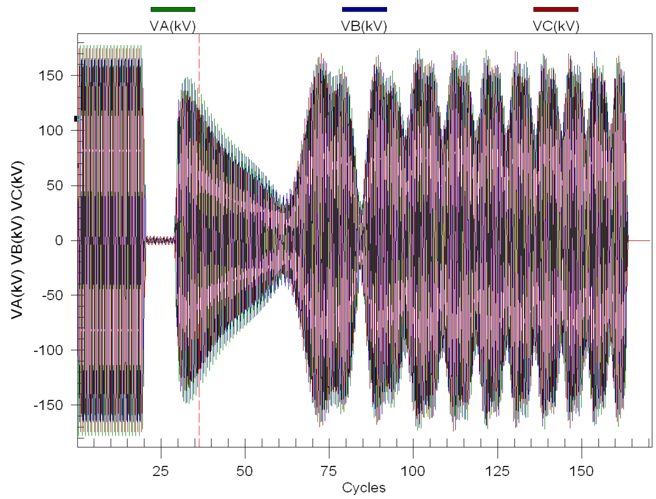

Fig. 15. Unstable power swing

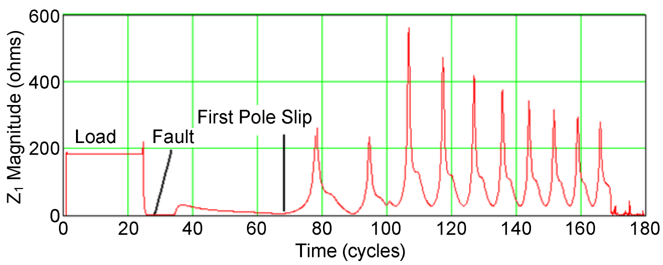

Fig. 16. Impedance plot for the unstable power swing

The system parameters that are needed to make settings calculations are shown in Table I.

TABLE I
POWER SYSTEM SIMULATION MODEL DETAILS

Parameter	Value
L1 positive-sequence impedance	18.86∠87.19° ohms
Relay current transformer ratio	3000:1
Relay voltage transformer ratio	3000:1
Load impedance	180 ohms
Stable swing rate	1.2 Hz
Unstable swing rate	4.5–8.5 Hz

The dual-quadrilateral technique may require an extensive power system study to calculate the relay settings. Criteria such as maximum load, total system impedance, and the fastest possible swing rate need to be determined for each system.

The system is protected by three mho elements, where Zones 1 and 2 are forward and Zone 3 is reverse. Zone 1 is set at 80 percent of the line impedance or 15.08 ohms, and Zone 2 is set at 120 percent of the line impedance or 22.62 ohms.

The inner and outer blinders are selected with a few observations. First, the load must be considered. If the outer blinder is set too large and encroaches on the load, the PSB function will be in danger of operating during heavy load conditions. Second, the inner blinder must be set larger than the Zone 1 and Zone 2 and possibly larger than the Zone 4 mho elements that are supervised by the PSB element. Finally, the two blinders must be far enough apart to allow enough time to capture the fastest swing rate determined from the system study. The selection of the two impedances for the inner and outer blinders for this simulation meets all three criteria (see Fig. 17).

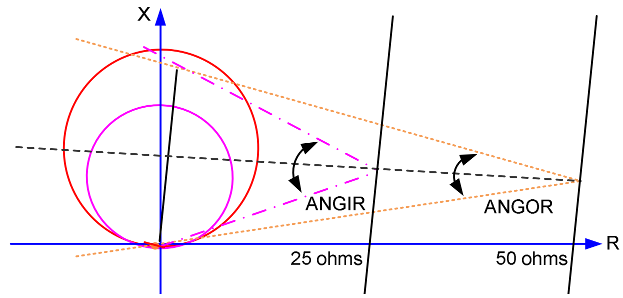

Fig. 17. Dual-quadrilateral settings calculation

From the equations in [6], the angle of the inner radius, ANGIR, and the angle of the outer radius, ANGOR, can be calculated. For this simulation, the inner radius and outer radius are 41.33 degrees and 21.36 degrees, respectively.

Next, the PSB delay is calculated and verified using the equation from [6]. The blocking delay is typically set from 1.5 to 2.5 cycles to give the relay a greater ability to detect the difference between a fault and an OOS condition [6]. For the simulation, the load is very large and the PSB element can tolerate a subcycle setting for this delay. The simulation uses a PSB delay of 0.61 cycles, or 10 milliseconds, to detect and block for an unstable swing that has a rate of approximately 5.5 Hz. The subcycle PSB delay was selected for demonstration purposes only. The relay has a processing interval of 2 milliseconds. This allows five counts to detect the power swing condition.

There are no settings associated with the SCV variation method; therefore, it does not require any power system studies in order to be applied properly.

The first simulation is a stable power swing for the dual-quadrilateral method. Fig. 18 shows the stable power swing and the PSB elements asserting as the impedance passes through the inner and outer blinders, X6ABC and X7ABC, respectively.

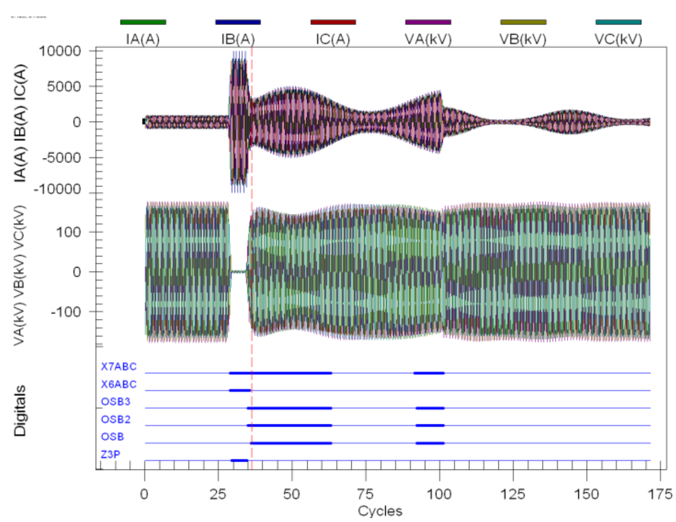

Fig. 18. Stable swing using the dual-quadrilateral technique

The results of the simulation for the SCV PSB method are shown in Fig. 19, Fig. 20, and Fig. 21. Both techniques detect the power swing condition and block accordingly.

The SCV method for detecting a power swing is slower than the dual-quadrilateral method. This is seen by comparing Fig. 18 with Fig. 19. It is slower because of the slow rate of change of the SCV. This is confirmed when studying Fig. 20.

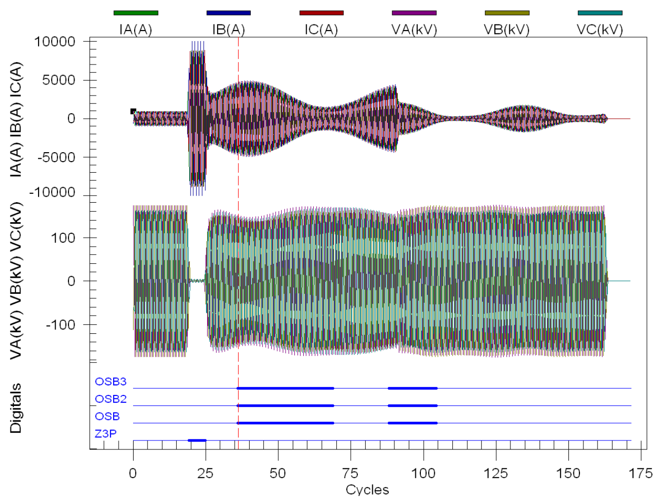

Fig. 19. Stable swing using the SCV technique

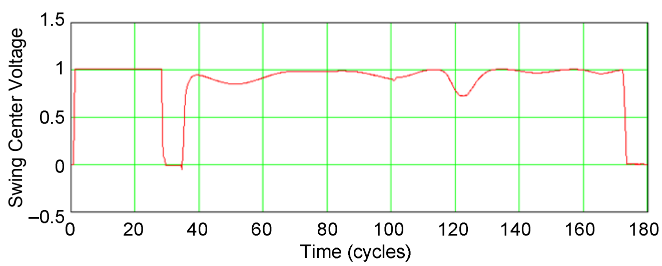

Fig. 20. SCV magnitude during the stable swing

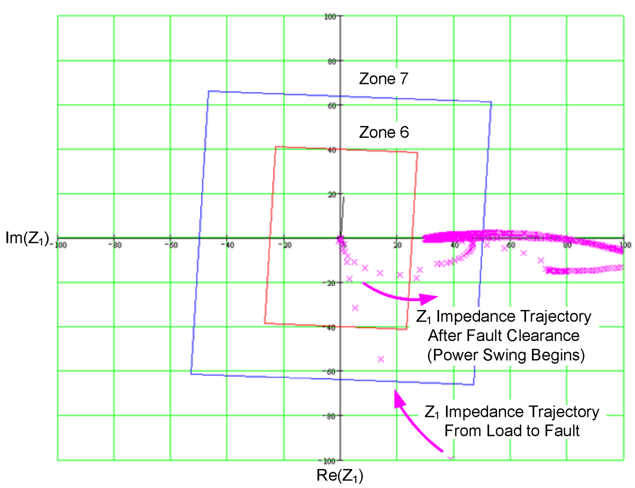

Fig. 21. Impedance plot of the stable power swing condition

The final simulations apply an unstable swing with an initial swing rate of 4.5 Hz and verify that the two methods operate similarly. Because the system was not set up for OST, the simulation focuses on the assertion of the PSB elements. The results of the unstable power swing using the dual-quadrilateral technique are shown in Fig. 22.

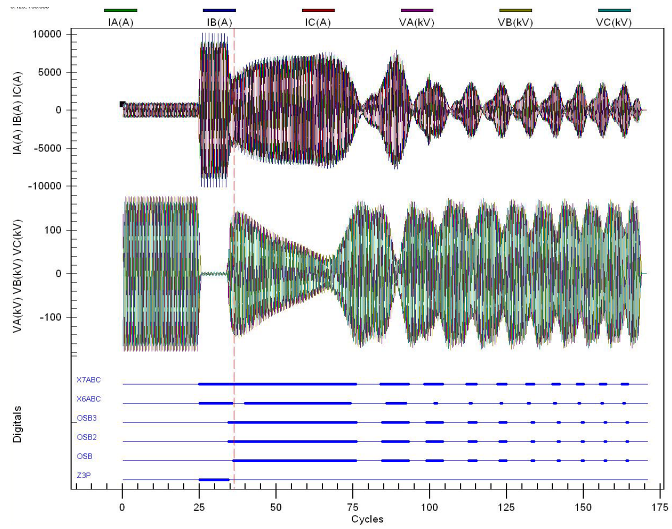

Fig. 22. Unstable swing using the dual-quadrilateral technique

Fig. 23, Fig. 24, and Fig. 25 show the results from the unstable power swing using the SCV method. Again, both techniques detect the power swing condition.

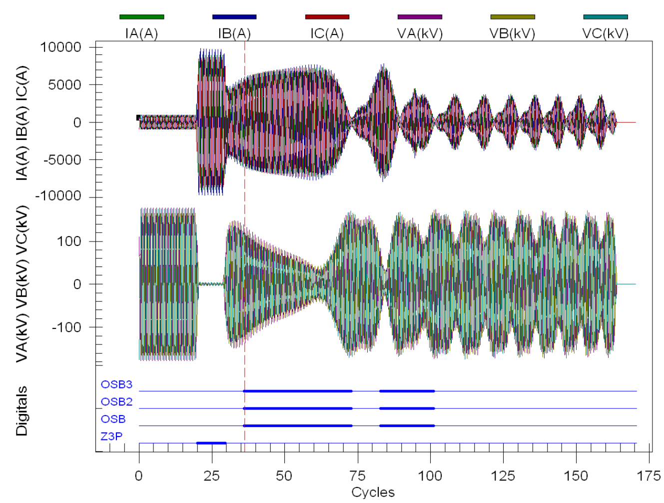

Fig. 23. Unstable swing using the SCV variation technique

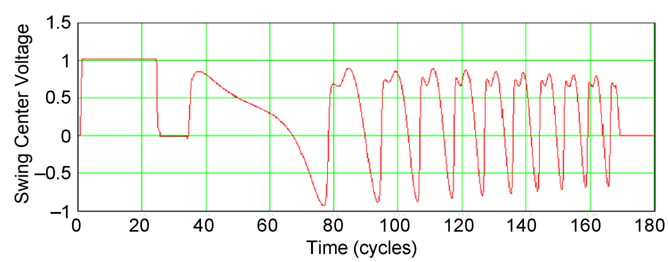

Fig. 24. SCV magnitude during the unstable swing

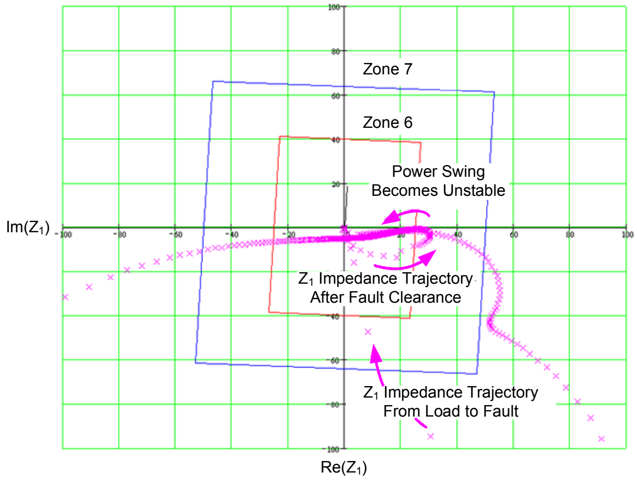

Fig. 25. Impedance plot of the unstable power swing condition

B. *Comparison Using Field Events*

1) *Example 1*

The first field event relates to a substantial power swing that took place on the network of a South American country in January 2005 and lasted for about 2 seconds. The event report ER 1 was recorded by the relay protecting a 76.67-kilometer, 120 kV transmission line with the following secondary impedance characteristics:

$$Z_1 = 2.05\angle 71° \text{ ohms}$$

$$Z_0 = 6.77\angle 72° \text{ ohms}$$

The line was protected by four mho elements covering Zones 1 through 4. Zones 2 and 3 were used in a directional comparison blocking (DCB) communications scheme. Zones 6 and 7 (quadrilateral blinders) were used for PSB detection following the principles of Method A. The minimum PSB delay to cross from Zone 7 to Zone 6 had been set at 2 cycles.

Fig. 26 shows the line voltages and currents recorded by ER 1 during the power swing. Fig. 27 shows the Z_1 impedance trajectory during the power swing.

Looking at Fig. 28 that shows the Z_1 trajectory crossing Zones 7 and 6, we can see that during the first crossing, the locus of Z_1 stayed in Zone 7 for 25 milliseconds (0.179 minus 0.154). Because the PSB delay was set to 2 cycles, the power swing could not be detected during the first crossing. During the second crossing of Zone 7, the Z_1 locus stayed in Zone 7 for 26 milliseconds (0.397 minus 0.371). Again, the power swing could not be detected, for the same reason. This example is therefore the classical situation where the speed of the Z_1 trajectory was not taken into account in the choice of the time settings.

In order to be able to detect this OOS condition, the solution is to expand Zone 7 so as to broaden the corridor between Zone 7 and Zone 6 and then provide more time to the Z_1 locus to stay inside Zone 7.

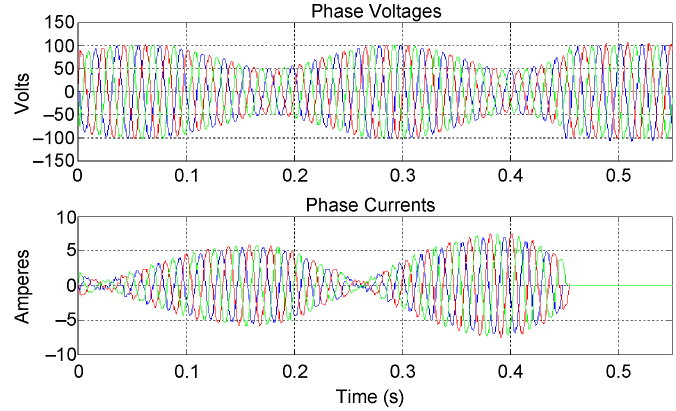

Fig. 26. Phase voltages and currents during the power swing for ER 1

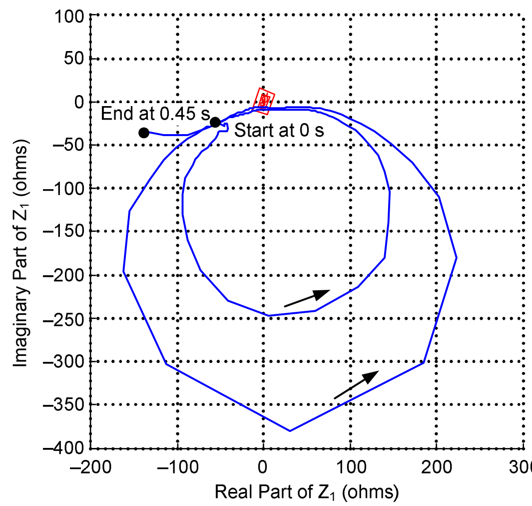

Fig. 27. Trajectory of Z_1 in the complex plane for ER 1

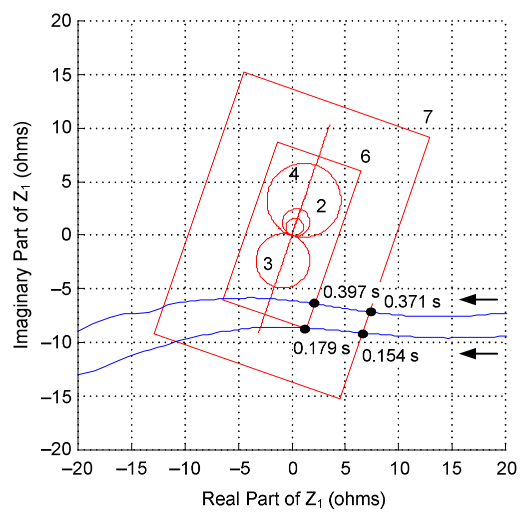

Fig. 28. Trajectory of Z_1 across Zones 6 and 7 for ER 1

Fig. 29 displays the PSB and mho element logic signals when the data were processed through a mathematical model of the relay that used the dual-quadrilateral technique (Method A). Because the power swing had not been detected, Zones 1, 2, and 4 (M1P, M2P, and M4P) operated during the event.

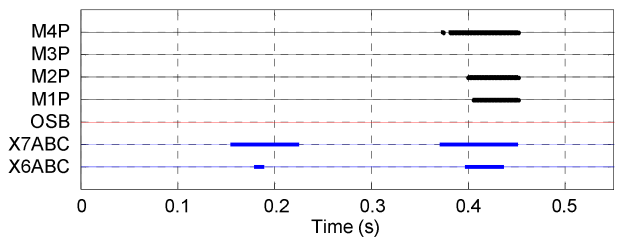

Fig. 29. OOS and phase mho logic signals for ER 1 (Method A)

Observe from Fig. 27 and Fig. 28 that the trajectory of the positive-sequence impedance did not traverse the forward-looking Zone 1, 2, or 4 distance elements. So why did these elements operate? The reason for their operation has to do with how these elements are polarized. The distance elements are polarized using positive-sequence memory voltage. The stiffness of the memory voltage is responsible for the assertion of forward-looking distance elements. In short, the frequency of the memory voltage polarizing signal and that of the operating signal do not correspond, resulting in the operation of the forward elements.

The event data were then processed by a mathematical model of the relay that uses the SCV technique (Method B). Fig. 30 shows the Z_1 trajectory entering the start zone. Because there is no delay in Method B associated with the crossing of the start zone as shown in Fig. 31, the power swing detection signal will assert as soon as the start zone has been crossed.

Fig. 32 shows the SCV1 together with the magnitude of the positive-sequence voltage. As shown in Fig. 31, the power swing is detected by the slope detector as soon as the Z_1 locus crosses the start zone. Had Method B been used in the original application, the line trip would have been avoided.

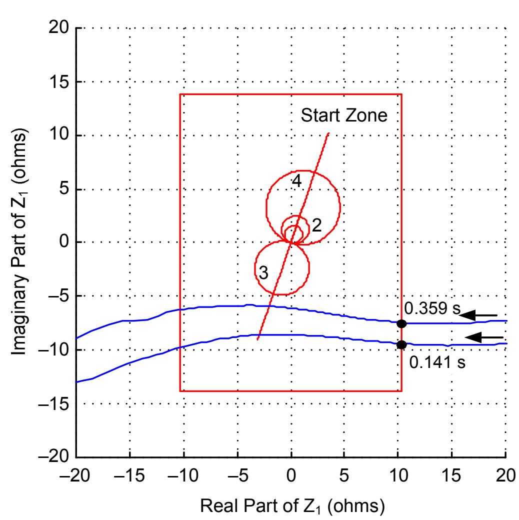

Fig. 30. Trajectory of Z_1 with respect to the start zone for ER 1 (Method B)

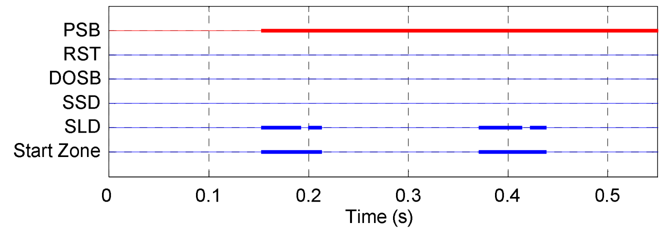

Fig. 31. OOS logic signals for ER 1 (Method B)

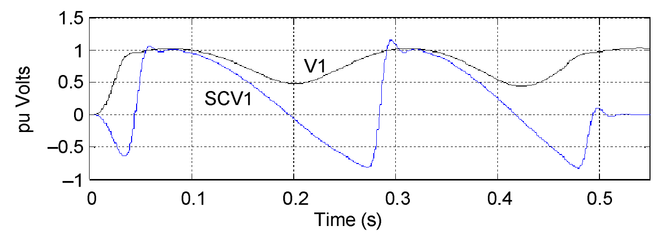

Fig. 32. Positive-sequence voltage magnitude and SCV1 for ER 1 (Method B)

2) *Example 2*

The second field event is from the same network as the first event and happened on the same day during the same power swing. The event report ER 2 was recorded by the relay protecting the adjacent 182.17-kilometer line and at the same voltage level as before, 120 kV. The line had the following secondary impedance characteristics:

$$Z_1 = 4.87\angle 71.2° \text{ ohms}$$

$$Z_0 = 16.08\angle 72.26° \text{ ohms}$$

The line had the same protection scheme as in the previous example.

Fig. 33 shows the line voltages and currents recorded by ER 2 during the power swing. Fig. 34 shows the Z_1 impedance trajectory during the power swing.

Looking at Fig. 35, we can see that the Z_1 trajectory simply did not cross Zones 7 or 6. It is therefore impossible in this case to detect the power swing with Method A and the settings selected by the user in the first place.

Fig. 36 displays the OOS and mho distance elements. From this, we can deduce that the mho phase distance element for Zones 1, 2, and 4 asserted during the power swing.

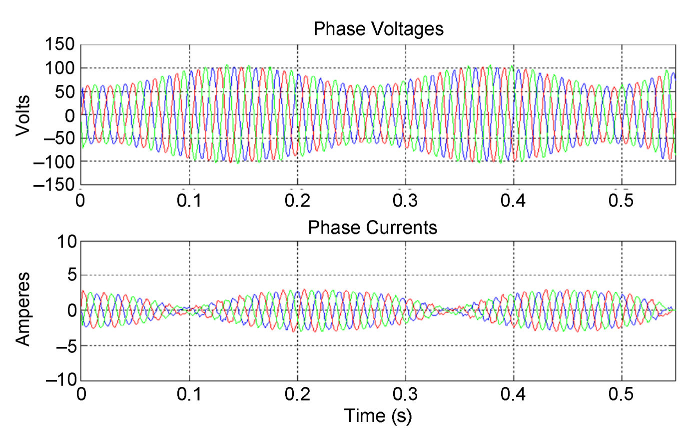

Fig. 33. Phase voltages and currents during the power swing for ER 2

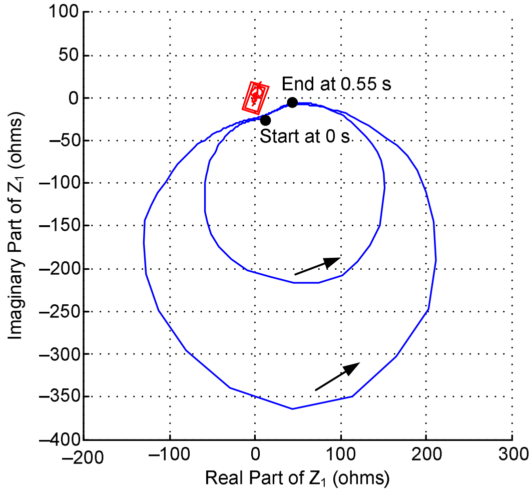

Fig. 34. Trajectory of Z_1 in the complex plane for ER 2

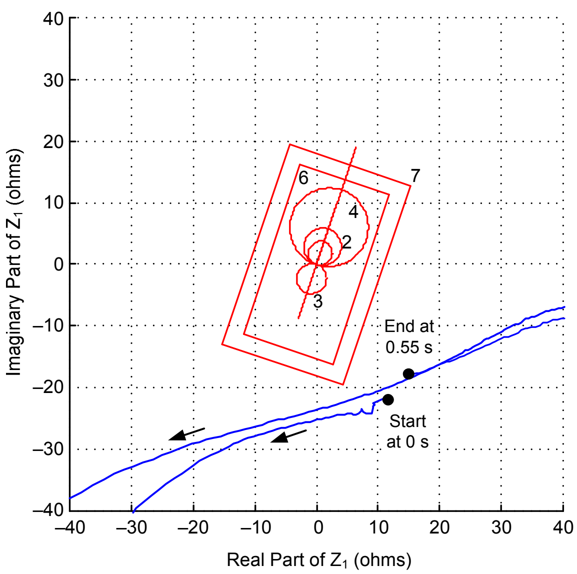

Fig. 35. Trajectory of Z_1 across Zones 6 and 7 for ER 2

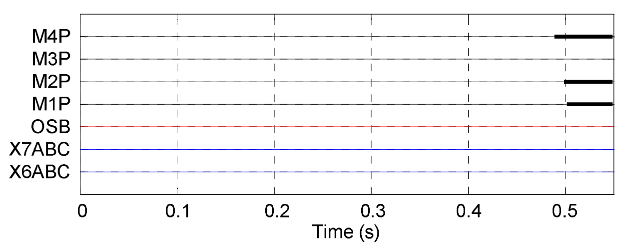

Fig. 36. OOS and phase mho logic signals for ER 2 (Method A)

In the same way as the previous example, the voltages of current waveforms were processed by a mathematical model implementing Method B. Fig. 37 shows the Z_1 trajectory entering the start zone. The crossing occurs at 0.24 second. The power swing detection signal will assert as soon as the start zone has been crossed.

Fig. 38 shows the SCV1 together with the magnitude of the positive-sequence voltage during the power swing. As shown in Fig. 39, the power swing is detected by the slope detector as soon as the Z_1 locus crosses the start zone. As in the previous example, if Method B had been used, the line trip would have been avoided.

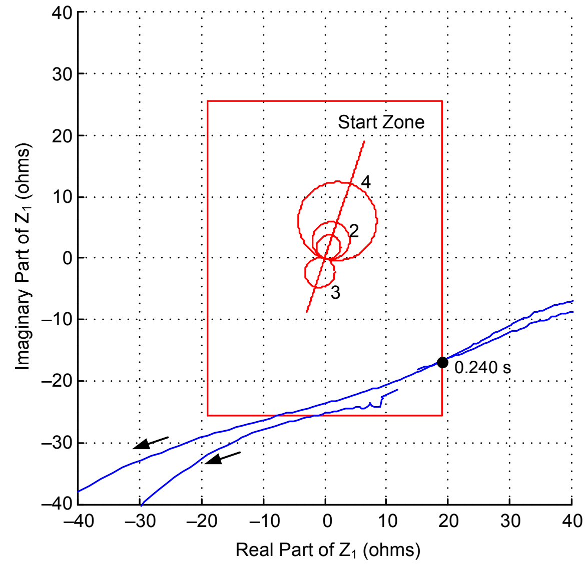

Fig. 37. Trajectory of Z_1 with respect to the start zone for ER 2 (Method B)

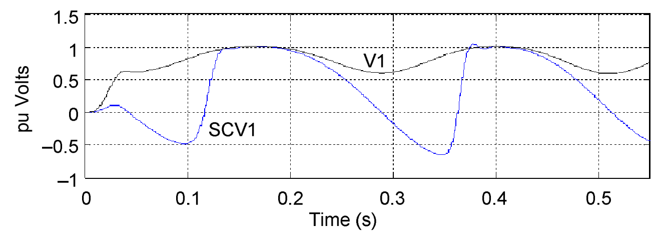

Fig. 38. Positive-sequence voltage magnitude and SCV1 for ER 2 (Method B)

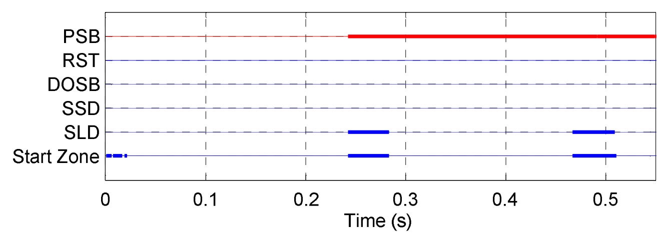

Fig. 39. OOS logic signals for ER 2 (Method B)

VI. Conclusion

This paper illustrates that two different methods can be used to successfully detect a power swing condition in a power system following a disturbance.

The first of these methods, the dual-quadrilateral method, requires an extensive study of the power system with faults applied during different operating conditions. The user has to analyze the trajectory of the Z_1 impedance in addition to the rate at which the Z_1 impedance traverses the Z_1 impedance plane. Using these data, the parameters for the inner and outer quadrilateral elements are established. The rate (speed) at which the Z_1 impedance traverses the Z_1 plane is used in determining the parameters of the PSB timer. This timer has to accommodate the fastest stable swing that the system may be subjected to, if out-of-step tripping for unstable swings is required. It is not always possible to set the quadrilateral elements and timers to coordinate properly, especially if the protected line is long and heavily loaded. For these cases, special measures have to be taken to ensure correct detection of a swing condition.

The second method is based on the SCV and is not dependent on any system source or line impedances (as shown in Section IV). Therefore, this method does not require any system studies to be conducted and, as such, does not require any user-defined settings.

This paper shows that both the dual-quadrilateral and the SCV methods can successfully be used to detect a power swing in a power system. Using field cases, the paper also illustrates that to successfully detect an OOS condition using the dual-quadrilateral method, the user must correctly set the quadrilateral element parameters, whereas the SCV method does not require the user to apply settings to the relay.

In conclusion, the SCV method allows the user to successfully apply power swing detection without any knowledge of the dynamic response of the power system.

VII. References

[1] C. R. Mason, *The Art and Science of Protective Relaying*. John Wiley & Sons, New York, 1956.

[2] N. Fischer, G. Benmouyal, and S. Samineni, “Tutorial on the Impact of the Synchronous Generator Model on Protection Studies,” proceedings of the 35th Annual Western Protective Relay Conference, Spokane, WA, October 2008.

[3] G. Benmouyal, D. Hou, and D. Tziouvaras, “Zero-Setting Power-Swing Blocking Protection,” proceedings of the 31st Annual Western Protective Relay Conference, Spokane, WA, October 2004.

[4] D. Hou, S. Chen, and S. Turner, “SEL-321-5 Relay Out-of-Step Logic,” SEL Application Guide (AG97-13), 2009. Available: http://www.selinc.com.

[5] IEEE Power System Relaying Committee WG D6, “Power Swing and Out-of-Step Considerations on Transmission Lines,” July 2005. Available: http://www.pes-psrc.org.

[6] J. Mooney and N. Fischer, “Application Guidelines for Power Swing Detection on Transmission Systems,” proceedings of the 32nd Annual Western Protective Relay Conference, Spokane, WA, October 2005.

[7] F. Ilar, “Innovations in the Detection of Power Swings in Electrical Networks,” Brown Boveri Publication CH-ES 35-30.10E, 1997.

VIII. Biographies

Normann Fischer received a Higher Diploma in Technology, with honors, from Witwatersrand Technikon, Johannesburg, in 1988, a BSEE, with honors, from the University of Cape Town in 1993, and an MSEE from the University of Idaho in 2005. He joined Eskom as a protection technician in 1984 and was a senior design engineer in the Eskom protection design department for three years. He then joined IST Energy as a senior design engineer in 1996. In 1999, he joined Schweitzer Engineering Laboratories, Inc. as a power engineer in the research and development division. Normann was a registered professional engineer in South Africa and a member of the South Africa Institute of Electrical Engineers. He is currently a member of IEEE and ASEE.

Gabriel Benmouyal, P.E., received his BASc in electrical engineering and his MASc in control engineering from Ecole Polytechnique, Université de Montréal, Canada. He then joined Hydro-Québec as an instrumentation and control specialist. He worked on different projects in the fields of substation control systems and dispatching centers. In 1978, he joined IREQ, where his main fields of activity were the application of microprocessors and digital techniques for substations and generating station control and protection systems. In 1997, he joined Schweitzer Engineering Laboratories, Inc. as a principal research engineer. Gabriel is a registered professional engineer in the Province of Québec and an IEEE senior member and has served on the Power System Relaying Committee since May 1989. He holds more than six patents and is the author or coauthor of several papers in the fields of signal processing and power network protection and control.

Daqing Hou received BSEE and MSEE degrees at the Northeast University, China, in 1981 and 1984, respectively. He received his PhD in Electrical and Computer Engineering at Washington State University in 1991. Since 1990, he has been with Schweitzer Engineering Laboratories, Inc., where he has held numerous positions, including development engineer, application engineer, research and development manager, and principal research engineer. He is currently the research and development technical director for East Asia. His work includes power system modeling, simulation, signal processing, and advanced protection algorithm design. His research interests include multivariable linear systems, system identification, and signal processing. Daqing holds multiple patents and has authored or coauthored many technical papers. He is a senior member of IEEE.

Demetrios Tziouvaras received a BSEE and MSEE from the University of New Mexico and Santa Clara University, respectively. He is an IEEE senior member and a member of the Power Engineering Society, the Power System Relaying Committee, and CIGRE. He joined Schweitzer Engineering Laboratories, Inc. in 1998 and currently holds the position of senior research engineer. From 1980 until 1998, he was with Pacific Gas and Electric, where he held various protection engineering positions, including principal protection engineer responsible for protection design standards, new technologies, and substation automation. He holds multiple patents and is the author or coauthor of many IEEE and protective relay conference papers. His work includes power system modeling, simulation, and design of advanced protection algorithms.

John Byrne-Finley received a BSEE and an MSEE with a power emphasis from the University of Idaho in 2007 and 2009, respectively. He joined Schweitzer Engineering Laboratories, Inc. in 2009 as an associate power engineer in the research and development division. John is a coauthor of several papers on electric vehicles and battery systems and is an active IEEE member.

Brian Smyth received a BS in general engineering with an electrical option and an MSEE from Montana Tech of the University of Montana in 2006 and 2008, respectively. He joined Montana Tech as a visiting professor in 2008 and taught classes in electrical circuits, electric machinery, instrumentation and controls, and power systems. He joined Schweitzer Engineering Laboratories, Inc. in 2009 as an associate power engineer in the research and development division. Brian is a coauthor of several papers on battery impedance measurement and is an active IEEE member.

Previously presented at the 2012 Texas A&M
Conference for Protective Relay Engineers.

20120315 • TP6552-01